Arthropod Structure & Development 86 (2025) 101428

Contents lists available at ScienceDirect

Arthropod Structure & Development

journal homepage: www.elsevier.com/locate/asd

Structure and variability in the female genital atrium of Uropodina (Acari: Parasitiformes)

Jeremy Naredo [a, *], J. Orlando Combita-Heredia [a], Thomas van de Kamp [b, c], Marcus Zuber [b], Elias Hamann [b], Ma. Magdalena Vázquez [d], Hans Klompen [a]

[a] Acarology Laboratory, Museum of Biological Diversity, Ohio State University, Columbus, OH, 43212, USA
[b] Institute for Photon Science and Synchrotron Radiation (IPS), Karlsruhe Institute of Technology (KIT), Hermann-von-Helmholtz-Platz 1, Eggenstein-Leopoldshafen, 76344, Germany
[c] Laboratory for Applications of Synchrotron Radiation (LAS), Karlsruhe Institute of Technology (KIT), Kaiserstr. 12, 76131, Karlsruhe, Germany
[d] Universidad de Quintana Roo, Av. Boulevard Bahía S / N Col. Del Bosque, CP 77009, Chetumal Quintana Roo, Mexico

ARTICLE INFO

Article history:
Received 12 December 2024
Received in revised form
18 February 2025
Accepted 25 February 2025
Available online 28 March 2025

Handling Editor: Dr G. Scholtz

Keywords:
Synchrotron X-ray microtomography
Uropodina
Genital atrium

ABSTRACT

Primary and secondary sexual characters of Mesostigmata are often used in species descriptions and phylogenetic analyses. The use of these characters has been focused almost exclusively on external structures. Digital 3D reconstruction based on synchrotron X-ray microtomography (SR-μCT) data allowed a comparative investigation of the structure of an internal system, the female genital atrium, in the mite lineage Uropodina (Parasitiformes: Mesostigmata). Despite substantial variability in observed structures, a general model for the endogynium, vagina, and muscle structure has been generated using a combination of SR-μCT and light microscopy. Most of the variations are hypothesized as related to species recognition and/or manipulation of the endospermatophore. The recorded variability may have substantial phylogenetic value, as a previously unreported modification of the vagina appears to diagnose a substantial lineage of "higher" Uropodina. This set of observations also support the hypothesis that the large family Urodinychidae is polyphyletic. Overall, SR-μCT and 3D reconstruction turned out to be very helpful for studies on internal organ systems in these very small organisms, lessening the need for laborious dissections or extensive Transmission electron microscopy-based investigations.

1. Introduction

Mites in the order Mesostigmata often show distinct sexual dimorphism in adults which allows use of sex-specific characters for species description and morphological analyses. Dimorphic characters include both primary (directly associated with gamete production or sperm transfer) and secondary structures (differences in shield structure, leg spines, etc.). Use of these characters has largely been restricted to external features and a few internal structures in females of lightly sclerotized species (e.g. the spermathecal structure in Phytoseioidea (Alberti and Di Palma, 2002)). Limitations of standard microscopy techniques leave internal structures under-utilized in descriptions and analyses, even though it has been shown that internal sex-specific structures can be very complex, as in e.g. *Megalolaelaps* (Cómbita-Heredia et al., 2021). Therefore, such structures may be a rich source of new information for further comparative studies.

Among secondary structures, a major focus has been on male cheliceral morphology in podospermous taxa (Alberti and Coons, 1999; Di Palma et al., 2009), that is species where sperm is transferred to the female using a highly modified structure (spermatodactyl) on the male chelicera. Females in these groups often show a pair of secondary sperm induction pores, with the primary genital opening used solely for oviposition. Other mesostigmatic lineages retain the ancestral mode of sperm transfer for parasitiform mites. Males produce a spermatophore which is transferred directly to the primary genital opening of the female using the male's chelicera, a process known as tocospermy. Males in tocospermous taxa do not show any obvious modifications of the chelicera, but modifications can be extensive for females, especially associated with the genital atrium, a chamber-like structure dorsal to the female genital shield (Michael, 1890; Alberti and Coons, 1999; Alberti et al., 1999). The atrium may feature a variety of rods, spines, and protrusions, collectively designated as the endogynium, that can be species

* Corresponding author.
E-mail address: naredo.1@osu.edu (J. Naredo).

https://doi.org/10.1016/j.asd.2025.101428

specific. Endogynial features have been used for species level identification in Parasitidae (Bhattacharyya, 1963), Diplogyniidae (Trägårdh, 1950; Kazemi et al., 2008), and some Uropodina (especially Trachyuropodidae) (Hirschmann, 1976a, 1976b, 1976c, 1976d, Hirschmann, 1976e; Hirschmann, 1976g; Hirschmann, 1976h; Hirschmann, 1976i).

The focus for this study is on the endogynium and genital atrium in Uropodina. Preliminary data suggested substantial variation in elements of the endogynial structures in Uropodina, but both the extent of this variability and its potential use as a source of characters in phylogenetic analyses are still unclear. Documentation of endogynial structures is complicated because they are internal and three-dimensional (3-D). Inferring 3-D structures from standard slide mounted specimens can be quite difficult, and technologies such as Scanning Electron Microscopy (SEM), which have been extremely useful in acarine taxonomy, are not effective for internal structures. Transmission Electron Microscopy (TEM) is still the gold standard for anatomy, but it requires great expertise and is very time intensive. New technologies, such as confocal microscopy and micro-CT, combined with generation of 3D reconstructions, may be a good alternative for the study of structures like the endogynium.

Synchrotron X-ray microtomography (SR-μCT) has been proven to be an excellent non-destructive tool for examining internal structures for smaller arthropods (Faulwetter et al., 2013; Keklikoglou et al., 2021). Tomograms allow digital analysis and the creation of interactive 3D reconstructions, thus providing a good understanding of the interactions of external and internal structures. Synchrotron light sources offer a much higher flux density and coherence than laboratory X-ray. Thus, acquisition times per sample can be reduced to below 1 min, even at micrometer spatial resolution (van de Kamp et al., 2018, 2022). Moreover, phase contrast options enable enhancing soft tissue contrast. Scanning a set of uropodine mites (Table 1) using SR-μCT allowed us to create digital 3D reconstructions of external and internal morphology, including the endogynium.

The primary aim of this study is to document the general structure and variability of the female genital atrium across Uropodina using a combination of SR-μCT and light microscopy. This is the first application of these techniques to mesostigmatic mites. Second, and based on the results of the primary aim, we discuss various hypotheses on the function of the internal genital structures relative to mating and oviposition.

2. Material and methods

Specimen collection and preparation. The taxa examined are listed in Table I. Whole mite samples were preserved in 95 % ethanol before processing. One batch of samples (15) were not stained, while a second batch (33) was stained by placing specimens for 24 h in a solution of 1 % iodine diluted in methanol (Metscher, 2009). After staining, the specimens were transferred back to 95 % ethanol for shipping and imaging. When dealing with extant arthropods, the best results can be obtained by performing SR-μCT while the samples are in ethanol (Lieberman et al., 2022; van de Kamp et al., 2022; Boudinot et al., 2024; Meira et al., 2024), thus profiting from optimal sample preservation.

High-throughput synchrotron X-ray microtomography was performed at the IPS Imaging Cluster of KIT Light Source using a parallel polychromatic X-ray beam generated by a 1.5 T bending magnet, spectrally filtered by 0.5 mm aluminum to remove low energy components from the beam. The resulting spectrum peaked at about 17 keV and had a full width at half maximum of about 10 keV.

The mites were scanned at magnifications of 5× (*Rotundabaloghia*; OSAL 110471) or 10x (all other samples), resulting in effective pixel sizes of 2.44 μm and 1.22 μm respectively. An air-bearing rotary stage (RT150S, LAB Motion Systems) was used for sample rotation. A fast indirect detector system consisting of a scintillator (5x: 25 μm LSO:Tb; 10x: 13 μm LSO:Tb (Cecilia et al., 2011);), a double objective white beam microscope (Optique Peter) (Douissard et al., 2012), and a 12-bit pco.dimax high-speed camera (Excelitas PCO GmbH) with 2016 × 2016 pixels was used. For each scan, 200 dark-field images, 200 flat-field images and 3000 equiangularly spaced radiographic projections were acquired in a range of 180° at 70 fps, resulting in a scan duration of approximately 43 s.

The 'concert' control system (Vogelgesang et al., 2016) was used for automated data acquisition and online reconstruction of tomographic slices for data quality assurance. Online and final data processing included dark and flat field correction and, if necessary, phase retrieval of the projections based on the transport of intensity equation (Paganin et al., 2002). Pipeline execution, including online tomographic reconstruction, was performed using the UFO framework (Vogelgesang et al., 2012). The final 3D tomographic reconstruction was done with tofu (Faragó et al., 2022) and additionally included ring removal, 8-bit conversion, and blending of the phase and absorption 3D reconstructions.

Volumetric data cropping. Fiji (Schindelin et al., 2012) was used to crop out the female specimen's volumetric data from the raw files. The cropped volumes were rotated virtually since storage in tubes with alcohol during scanning did not allow for proper alignment of the specimens. This was also done in Fiji by re-slicing the stack data from different axes followed by rotation for proper alignment.

Segmentation. Segmentation involves the partitioning of the volumetric image data using ‘tags’ to extract regions of interest from the rest of the 3D image. It requires knowledge of the different ‘segments’ that need to be isolated from the original data. Since the purpose of this study is to describe the structure and variability in the genital atrium of Uropodina, we used illustrations (Fig. 1) and descriptions of Michael (1890) as the basis for the different structures/segments. Cropped and rotated data were analyzed in Slicer3D version 5.6 (Fedorov et al., 2012) to locate reproductive structures and capture 2d images of them in 3 different axes as reference for segmentation. In some cases, we also captured 3D renderings of the cropped volume to expose the internal genital structures in 3D.

Segmentation of volumetric images can be done manually by tagging each stack/slice of images with distinct colors to represent different structures. However, several programs are available for automatic segmentation including built-in algorithms within Slicer3D. Since mite organs are separated by gaps as small as 1 micron, which translates to 1 pixel for our data, interpolation by these methods was not effective. To overcome this, we used the online program Biomedisa Version 24.5.22 (Lösel et al., 2020) for the semi-automated segmentation of the genital structures. The program takes information from pre-segmented slices then performs smart interpolation of the segment using the underlying image data. We first used MITK (Wolf et al., 2004) to segment about 3–10 % of the total number of slices as reference for the smart interpolation. The Biomedisa output in.nrrd format was manually corrected back in Slicer3D with help of the ‘edit in 3D view’ function.

Visualization and rendering. After manual correction of the segmentation in Slicer3D, polygon meshes were exported as individual.obj files including the relative position and rotation data. The files were imported and rendered in Blender 4.1 (Blender_Development_Team, 2024). Still images and rotating video or gif images were imported for visualization. Both still images of the rendering from Blender and x-ray images from Slicer3D were modified and edited in Adobe Photoshop (2024) to highlight or filter various structures.

Light Microscopy. Additional female specimens of the same

Table 1
Uropodine taxa with Micro-CT data used in comparative study of the female genital atrium.

Taxon name	Family	Voucher number	Nodus	Stained
Diarthrophallus quercus	Diarthrophallidae	OSAL 130264		yes
Polyaspis	Polyaspidae	OSAL 115649		
Acroseius	Trachytidae	OSAL 152494		yes
Afrotrachytes	Trachytidae	OSAL 152497		yes
Trachytes	Trachytidae	OSAL 115746		
Australocilliba	Cillibidae	OSAL 152495		yes
Laqueaturopoda laqueata	Cillibidae	OSAL 152487		yes
Discourella	Discourellidae	OSAL 129959		
Foveolaturopoda	Uropodidae	OSAL 152466		yes
Penicillaturopoda	Uropodidae	OSAL 152492		yes
Trachycilliba	Uropodidae	OSAL 152468		yes
Uropoda cornuata nr.	Uropodidae	OSAL 152496		yes
Metadinychus	Uropodidae	OSAL 110362		
Brasiluropoda	Brasiluropodidae	OSAL 152464	yes	yes
Cyllibula	Cyllibulidae	OSAL 152477	yes	yes
Dinychus micropunctatus	Dinychidae	OSAL 130263	yes	yes
Hexacoprnutophorus	Eutrachytidae	OSAL 152469	yes	yes
Loksaphorus	Eutrachytidae	OSAL 110350	yes	
Macrodinychus	Macrodinychidae	OSAL 115174	yes	
Macrodinychus sellnicki	Macrodinychidae	OSAL 152488	yes	yes
Nenteria longispinosa nr.	Nenteriidae	OSAL 152491	yes	yes
Chelonuropoda	Oplitidae	OSAL 152490	yes	yes
Oplitis	Oplitidae	OSAL 115400	yes	
Uroplitana moseri	Oplitidae	OSAL 152499	yes	yes
Rotundabaloghia	Rotundabaloghiidae	OSAL 110471	yes	
Tetrasejaspis	Tetrasejaspidae	OSAL 152489	yes	yes
Leonardiella whitkombi	Trachyuropodidae	OSAL 152498	yes	yes
Origmatrachys	Trachyuropodidae	OSAL 152493	yes	yes
Trichouropoda	Trematuridae	OSAL 115409	yes	
Trematurella lagunae cf.	Trematuridae	OSAL 152470	yes	yes
Circocylliba	Trichocyllibidae	OSAL 152474	yes	yes
Planodiscus burchelli	Trichocyllibidae	OSAL 152476	yes	yes
Trichocylliba	Trichocyllibidae	OSAL 115634	yes	
Trigonuropoda	Trigonuropodidae	OSAL 110445	yes	
Chiropturopoda	Uroactiniidae	OSAL 152483	yes	yes
Uroactinia	Uroactiniidae	OSAL 005913	yes	
Urodiaspis	Urodiaspidae	OSAL 152478	yes	yes
Allodinychus	Urodinychidae	OSAL 102371	yes	
Urosternella	Urodinychidae	OSAL 110444	yes	
Elegansovella	Urodinychidae	OSAL 152471	yes	yes
Micherdzinskiiobovella makilingensis	Urodinychidae	OSAL 152472	yes	yes
Uroobovella luzonensis	Urodinychidae	OSAL 152473	yes	yes

species and with the same collection data as those sent to KIT were processed for light microscopy at the Ohio State University Acarology laboratory (OSAL). Samples were cleared in lactic acid and imaged in both cavity slides in lactic acid and as semi-permanent slides made using Hoyer's medium. Images were generated using the automated Z-stacking feature of the Nikon NIS elements package on a Nikon Eclipse 90i™ (Nikon Incorporated, Melville, NY, USA) compound microscope with a PC controlled Ds-5M-U1 digital camera.

Terminology. Terminology of internal structures in the female genital area is confusing as the few authors dealing with these structures all seem to have their own preferred terminology. For this study we adopt most of the terminology of Woodring and Galbraith (1976), while noting alternative terms used by Michael (1889, 1890), Evans (1992), and Alberti and Coons (1999). Family classification of Uropodina follows Beaulieu et al. (2011), generic classification follows Kontschán (2024).

3. Background

The main elements of the primary genital system in female Uropodina are a single ovary, paired oviducts, a uterus, and a vagina (Woodring and Galbraith, 1976; Evans, 1992; Alberti and Coons, 1999). Michael (1890) referred to both uterus and vagina as "vagina", but most other authors distinguish the cuticle-lined vagina from the uterus. The vagina opens into the genital atrium (= vestibule of Michael (1889, 1890)), a space dorsal to the genital shield. The current study focusses on the genital atrium and its associated structures. Although multiple studies have noted structures dorsal to (= internal to) the female genital shield, few studies have followed up on the pioneering work of Michael (1889, 1890, 1894). The diversity of taxa studied is also remarkably small. Michael focused on three species he designated as *Uropoda krameri* (Canestrini), *U. ovalis* (Koch), and *U. vegetans* (De Geer). These most probably correspond to species currently classified as, respectively, *Leiodinychus orbicularis* (Koch), *Oodinychus ovalis*, and *Pseuduropoda vegetans*. All three of these species (assuming the identifications are correct) belong to the family Trematuridae. He added a few, and far less detailed, observations on *Cilliba cassidea* (Hermann) (Cillibidae) and *Glyphopsis formicariae* (Lubbock) (Trachyuropodidae). Finally, as part of a study on the anatomy of the entire idiosoma, Woodring and Galbraith (1976) added valuable data for *Fuscuropoda agitans* (Banks) (now *Uroactinia agitans*, Uroactiniidae). Other discussions on the genital atrium (Evans, 1992; Alberti and Coons, 1999) are almost entirely based on results from these studies.

As noted above, the genital atrium is situated dorsal to the female genital shield, which seals off the ventral exit of the female

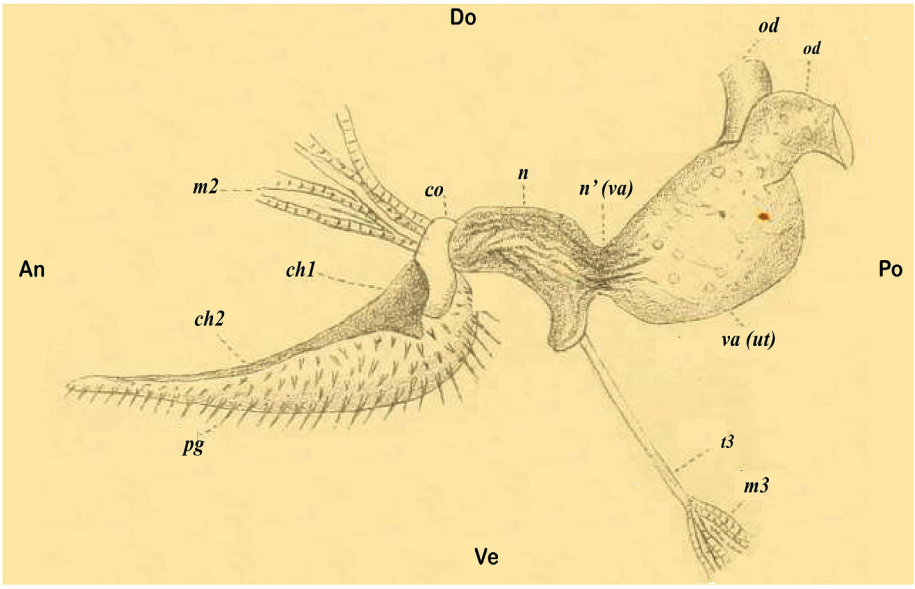

Fig. 1. Lateral view of internal genital system of *Oodinychus ovalis* (Koch) (adapted from Michael, 1890). Original abbreviations (updated designation): *ch1-2*: strengthening rods around sole and heel of endogynium; *co*: collar of chitin attached to heel of endogynium; *m2-3*: muscles; *n n'*: neck of vagina (vagina); *od*: oviduct; pg: perigynum (endogynium); *t3*: tendon; *va*: vagina (uterus). An (anterior), Po (posterior), Do (dorsal) and Ve (ventral) labels provided for general orientation.

genital system when closed completely. The genital shield hinges posteriorly. Within the atrium, a membranous structure is loosely attached to the inner surface of the genital shield (Michael, 1889). This forms the ventral lining of the atrium. The dorsal part of the atrium in both Trematuridae and *Uroactinia* is formed by the endogynium (= perigynum of Michael (1890), endogynum of Evans (1992)). Michael described the endogynium as "a lamina of chitinized tissue with sclerotized marginal support rods" (*ch* in Fig. 1). Our focus will be on these support rods, as they are very clear in micro-CT data. The endogynium (*pg*) in *Oodinychus ovalis* forms a structure vaguely resembling a shoe (Michael, 1890), with a "heel" (*ch2*) and a "sole" (*ch1*). Both are shaped by chitinous support rods forming a frame-like structure, often filled in by less sclerotized membranes. Notably, the support rods of the heel may or may not be fully fused with each other or with support rods for the sole. The membrane of the sole is often concave dorsally and convex ventrally. While the dorsal side appears smooth, the ventral side of the chitinized membrane may carry spine-like structures in varying patterns. The appearance of these structures can be species or lineage specific and is the only aspect of the atrial structures that is frequently recorded for at least some uropodine taxa, e.g. Trachyuropodidae (Fig. 10a–b). Laterally, a flexible membrane connects the sclerotized endogynium and the lateral margins of the genital shield. As a result, access to (spermatophore introduction), or egress from (oviposition) the genital atrium is limited to the anterior opening, even when the genital shield is fully opened (Woodring and Galbraith, 1976). At rest, Michael (1890) noted that the endogynium almosts rests on the inside lining of the genital shield, with the lateral membrane rising upward from the endogynium. The genital atrium is therefore not a "chamber" at all times. It only becomes a chamber during oviposition and spermatophore introduction, during which times the genital shield opens, and the atrium roof gets raised (Michael, 1890; Woodring and Galbraith, 1976). Two different mechanisms for raising the roof of the genital atrium have been proposed: Woodring and Galbraith (1976) hypothesized that the roof of the atrium gets raised by release of hemolymph pressure, while Michael (1890) proposed action by muscles attached to the sclerotized support rods of the endogynium's heel. The above description is based on *O. ovalis*, but largely matches the structures recorded for *L. orbicularis*, *P. vegetans*, and *U. agitans*.

Additional structures include a seminal receptacle (ventral to the vagina in *O. ovalis*), a pair of accessory glands opening in the atrium, and various muscles. Even within his relatively small taxon sample, Michael (1890) noted variability in the seminal receptacle and accessory glands. For example, the receptacle was absent in *L. orbicularis*, single in *C. cassidea* (and *U. agitans*), and paired in *P. vegetans*, and accessory glands were elongate (*O. ovalis*) or roundish (*P. vegetans*).

4. Results

4.1. Endogynium

Micro-CT data recovered most of the organs and structures related to the reproductive system of the females described in previous works. Default x-ray views in Slicer3D allowed observation of soft tissues (uterus, paired oviducts, and ovary) but the technique worked substantially better with well-sclerotized structures and muscles (Fig. 2). The membranes connected to the sclerotized structures were also hard to recognize due to their nature and the fact that they are folded at rest. In instances where the scanned mites had their genital shield open, allowing the membranes to expand, the membranes become too thin to be detected. Hence, the following results from micro-CT data focus on sclerotized structures and associated muscles.

Based on a comparative study across a wide range of uropodid taxa, we recognize two separate elements in the endogynium, each related to a particular muscle. Muscle *m2,* which originates from the dorsal shield, is attached to a sclerotized structure at the antero-dorsal side of the vagina (hereby, *endogynium 1*). On the other hand, muscle *m3,* which originates from near the lateral sides of the anal opening, terminates at the antero-ventral side of the vagina (*endogynium 2*). These designations should not be confused with Michael's "heel and sole" of the endogynium (*ch1 & ch2*, Fig. 1). The distinction between the two elements is not obvious in

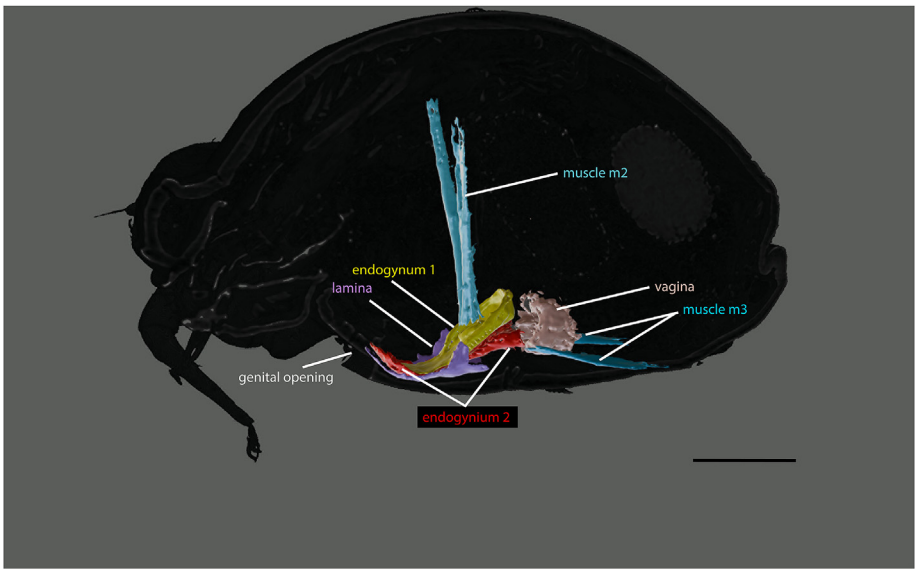

Fig. 2. Lateral section of female *Uropoda cornuata* Kontschan with tagged structures of the female reproductive system. Scale bar: 100 μm.

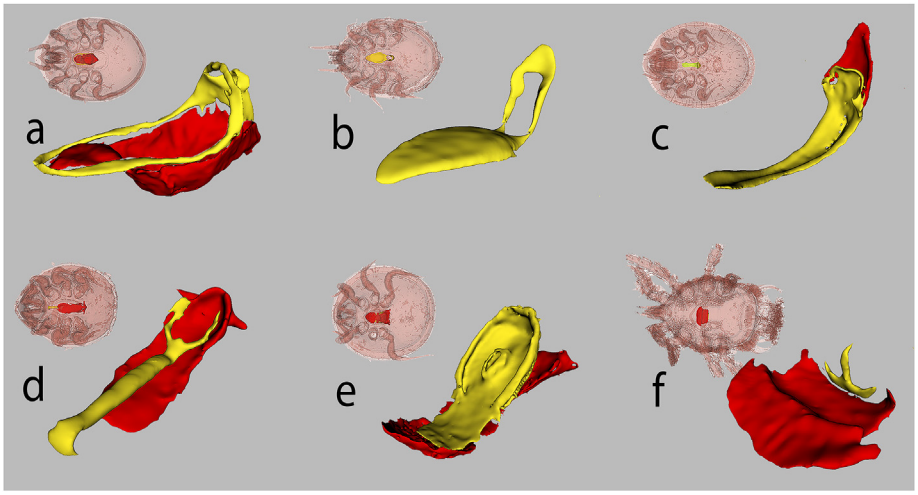

Fig. 3. The different types of endogynium in female Uropodina. Type 1: a, *Chiropturopoda* and b, *Nenteria*; Type 2: c, *Cyllibula*; Type 3: d, *Uropoda* and e, *Penicillaturopoda*; Type 4: f, *Afrotrachytes*. Yellow: endogynium 1; red: endogynium 2. Habitus (translucent pink) of each female included to show size and position of the endogynium relative to the body.

most species but is based on observations in *Uropoda cornuata* Kontschan (Fig. 2) where the two are clearly separated. We use the hypothesis of two separate elements as the basis for interpretation of the following observations.

For most species, endogynium 1 comprises most of what Michael pointed out as the “shoe” with recognizable heel and sole components, while endogynium 2 may be considered synonymous to Michael's perigynum (*pg*, Fig. 1). In some cases, the combination of the two endogynial components forms a complete genital chamber. Variation in shape and level of development of the endogyniums 1 and 2 can define the types of endogyniums in female Uropodina enumerated below.

The standard (type 1) (Figs. 1 and 3a-b). Many Uropodina fit with the generalized endogynium (shoe) model as proposed by Michael (Fig. 1). In this type, endogynium 1 comprises the heel and sole with variation in shape between taxa examined. Endogynium 2 is reduced to a thin membrane and sometimes inconspicuous (Fig. 1, pg). Consistent with Michael's observations, the heel of the endogynium is positioned directly anterior to the opening of the vagina.

The heel portion can appear to consist of rods only or can be arranged like a wishbone (two strong rods fused dorsally at an angle of 70–90°) as shown in *Chiropturopoda* (Fig. 3a), *Uroactinia, Urosternella*, and *Uroobovella luzonensis* Hiramatsu and Hirschmann. In these species, the two sclerotized rods continue anteriorly and fuse medially to form a hollow sole. The overall hollow sole surrounds and supports the spine-bearing chitinized membrane. The heel can also appear like a horseshoe with a rounded top as seen in *Nenteria* (Fig. 3b), *Trematurella, Trichouropoda, Brasiluropoda, Oplitis, Chelonuropoda*, and *Allodinychus*. In these species the anterior half of the endogynium (sole) appears as a completely sclerotized region from the lateral margins to the center. Endogynium 2 seems absent in *Nenteria, Allodinychus,* and *Trichouropoda*, and reduced in *Brasiluropoda*.

Type 2 (Fig. 3c). This type of endogynium has been observed in *Cyllibula* (Fig. 3c), *Trichocylliba, Planodiscus, Circocylliba,* and to some extent in *Depressorotunda*. The endogynium of this type appears as a highly curved shoe, with two closely positioned rods that

sometimes (e.g. *Trichocylliba*) fuse midway through the length of the endogynium into a single rod. Endogynium 2 is reduced to less than a third the size of the entire endogynium but appears to be what comprises the endogynium's heel in *Cyllibula*.

Type 3 (Figs. 2 and 3d–e). This type of endogynium was observed in species in the family Uropodidae (*Uropoda, Pennicilaturopoda, Metadinychus*) and Dinychidae (*Dinychus*). In this type of endogynium the two components are mostly of equal size and development, although very variable in their shape and position. The endogynial structure of this type still resembles a shoe but most of the heel part is composed of endogynium 1 while the sole is made up of endogynium 2. In all these species, endogynium 2 forms the ventral base of the whole endogynium, spanning the length of the genital shield, and is as wide as the vagina itself. In both *Uropoda* and *Pennicilaturopoda*, the heel's posterior margins point out to the sides (red in Fig. 3dand e). However, the shape of the heel can be more variable and can resemble those of species with type 1. In *Uropoda* (also in *Dinychus* and *Foveolaturopoda*), the heel takes the shape of a horseshoe but in between the rods is a sclerotized membrane that extends slightly further anteriorly (Fig. 3e, yellow). In *Penicillaturopoda*, and in *Metadinychus* the lateral rods of the heel in endogynium 1 fuse medially and extend as a single rod (Fig. 3d, yellow).

Type 4 (Fig. 3f). This type has been observed in species from more 'basal' uropodines (*Afrotrachytes, Acroseius, Polyaspis*, *Trachytes*). In these species, endogynium 1 is reduced to a triangular or slim pointy rod, directly anterior of the vagina as in *Afrotrachytes* (red in Fig. 3f). Endogynium 2 is situated just below (antero-ventral to) the opening of the vagina and extends anteriorly and laterally almost taking the shape and size of the genital shield.

Alternative system (type 5). The endogynium in females of some taxa is absent or very poorly developed, but in most of these taxa (except for *Diarthrophallus* and *Tetrasejaspis*), females show a very unusual modification of the vagina: oval with uniform-sized spine-like structures on its exterior (Figs. 4 and 5). The spine-like folds originate from a central sclerotized cylindrical structure, which we hypothesize is a modified endogynium 2. The tube-like endogynium 2 expands to a wider opening anteriorly with a wider ventral side. The spiky external structure is reminiscent of a durian fruit and will be designated as a "durian-style" vagina. The spine-like structures appear to be modified folds (Fig. 5), suggesting that this part of the vagina could expand (see below). This type of vagina was observed in females of *Trigonuropoda* (Trigonuropodidae), *Hexacornutophorus*, *Loksaphorus* (Eutrachytidae), and a few genera of Urodinychidae (*Elegansovella*, *Micherdzinskiiobovella*, *Monstrobovella*). Interestingly, the structure was also observed in *Laqueaturopoda* (Cillibidae), though the internal tube-like structure (endogynium 2) in this taxon appears to be inverted with the anterior opening being wider on the dorsal side.

A pair of sclerotized rods reminiscent of the "heel" structure of the endogynium lies anterior to the vagina and just above the genital lamina and shield. The rods form a V-shape, converging at their posterior end, while diverging at their anterior end, extending up to the midpoint of the genital shield. At the anterior tip of the rods is a loop which makes the structures look like a pair of sewing needles (Fig. 10c–e, red arrows). The rods are connected to the membranes surrounding the genital atrium. They are hypothesized to be part of endogynium 1.

A balloon-like structure was observed in genera that have the durian-type vagina. In some taxa, it was positioned dorsal to the vagina, in others ventral to the vagina. We suspect that this is an inflated sperm receptacle. In cases where the structure is positioned above the vagina, a membranous tube connects it to the vagina.

The vaginal structure in the ant-parasitoid genus *Macrodinychus* shares some elements with taxa having a durian-type vagina but differs in other respects (Fig. 6). For example, the vagina is reinforced with a cylindrical tube (endogynium 2), but the spine-like folds noted for the durian-type are absent. The anterior half of the cylinder extends further anteriorly from the vagina into the genital chamber and forms a tongue-like structure. Another similarity is the presence of paired rods (endogynium 1) associated with membranes of the genital atrium. In *Macrodinychus* the rods are far apart posteriorly but are angled inwards anteriorly (Fig. 6b). The rods appear to secure the position of the balloon-like sperm receptacle organ which is positioned on top of the vagina (Fig. 6c). A lateral section of the specimen reveals that this sperm receptacle connects to the vagina through the cylindrical reinforcement (Fig. 6c).

4.2. Musculature

The musculature of the female genital region in Uropodina (Michael, 1890; Woodring and Galbraith, 1976) corresponds well

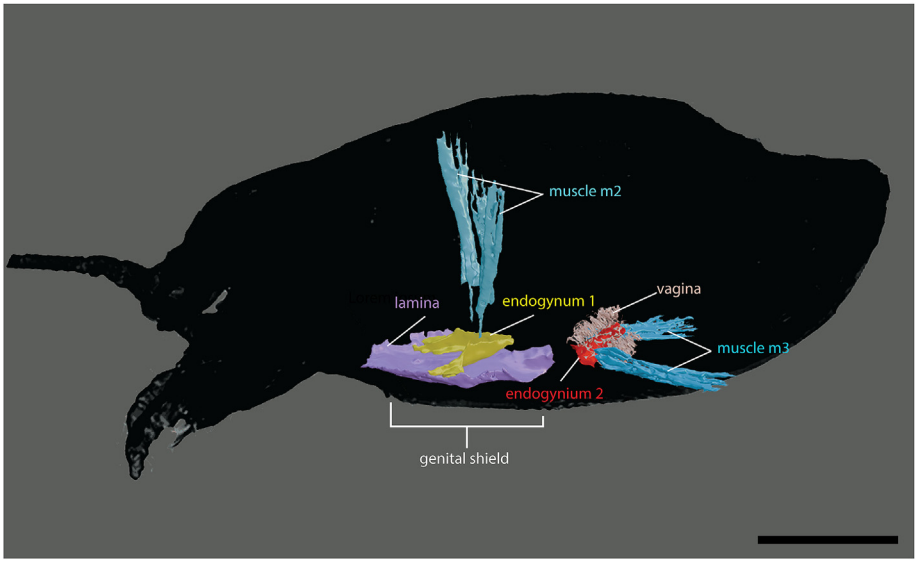

Fig. 4. Lateral section of a female *Trigonuropoda* sp., showing tagged (colored) muscles and organs of the reproductive system. Scale bar: 100 μm.

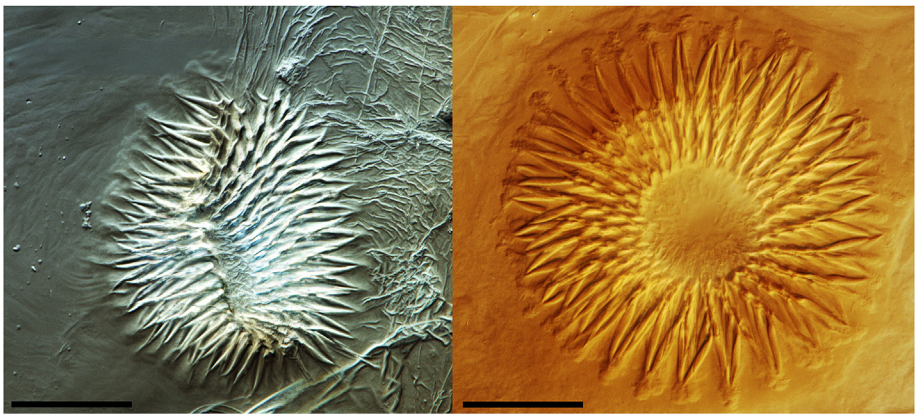

Fig. 5. Photomicrographs of the durian-type vagina of *Trigonuropoda* sp. showing the intricate spine-like folding pattern. Lateral (left; OSAL 118042) and cross section (right; OSAL 160732) views. 1000× magnification. Scale bars: 25 μm.

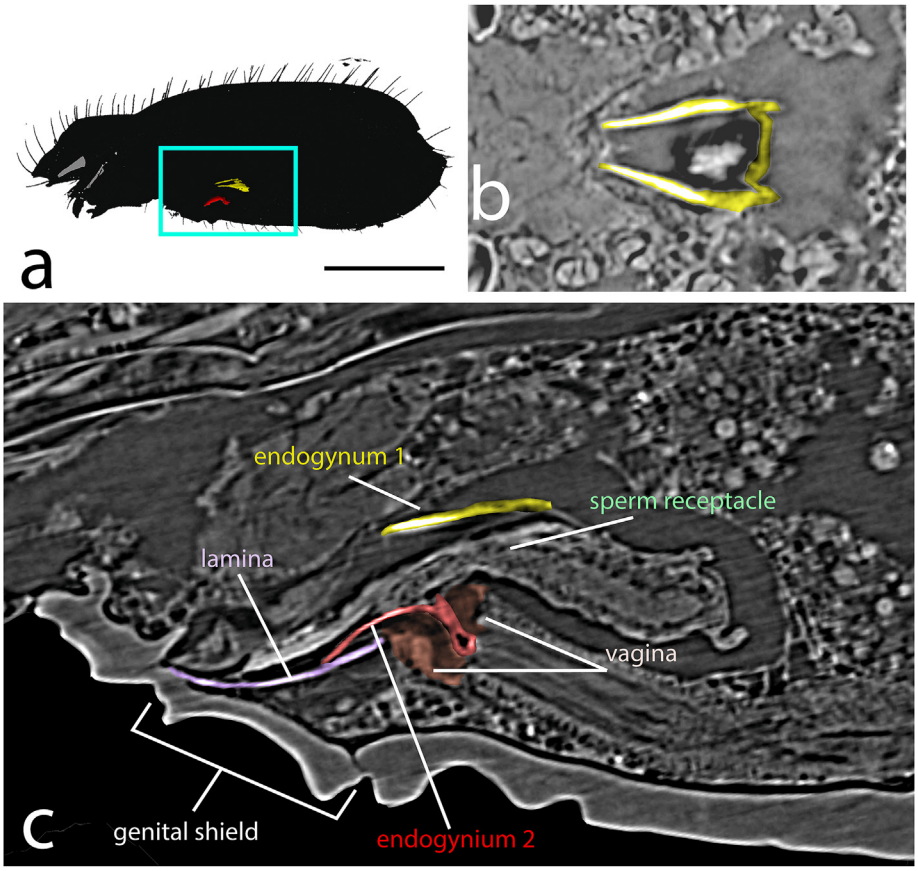

Fig. 6. *Macrodinychus sellnicki* Hirschmann and Zirngiebl-Nicol, female. a, silhouette of habitus showing relative position of endogynium 1 and 2 (box). Scale bar: 250 μm; b, dorsal view revealing paired bars of endogynium 1; c, lateral view of the boxed region showing position of endogyniums 1 and 2 relative to other parts of the genital atrium.

with that recorded in Gamasina (Akimov and Yastrebtsov, 1988) with three main muscles. Michael (1890) recognized a fourth muscle (his *m4*) inserted on the seminal vesicle. Of these muscles, Michael's occlusor muscles of the genital plate, *m1*, (muscles of genital valve (*mge*) of Akimov and Yastrebsov, genital plate muscles (*Mg*) of Woodring and Galbraith) are inserted laterally on the genital shield at about 1/3 from the posterior end of that shield. Their origins are on the posterior part of the dorsal shield. These muscles function to keep the genital shield closed. The genital shield opens by relaxation of this muscle pair.

Muscle pair *m2* (levator muscle of the perigynum of Micheal, dilators of the vaginal cavity (*mva1*) of Akimov and Yastrebtsov, vaginal support muscles (*Mv*) of Woodring and Galbraith) insert on the heel of the endogynium (if present) or dorsally on the basal end of the vagina in taxa without a distinct endogynium (Fig. 7). Their origins are on the endosternite (Fig. 8a, b, e) or directly on the dorsal shield (Fig. 8c, d, f). Which origin is used appears to depend on the development of the endosternite. Functionally, in taxa with a complete endogynium (types 1–4) these muscles raise the endogynium to expand the genital atrium from its folded resting form. In

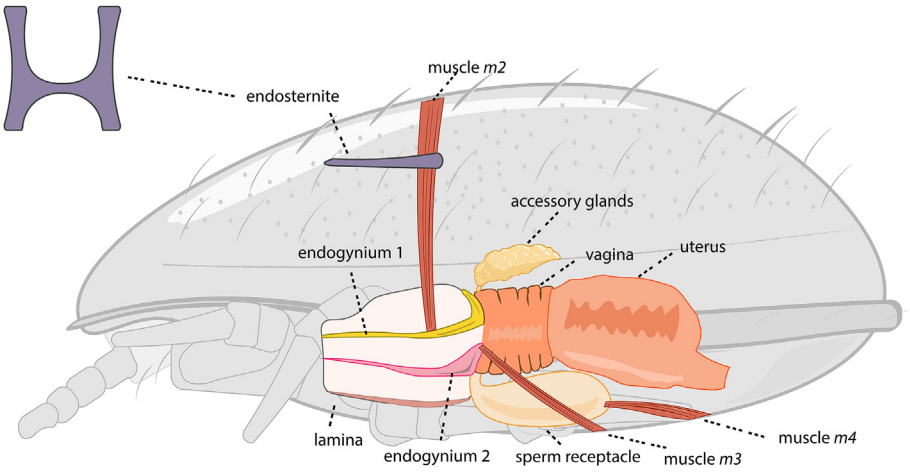

Fig. 7. Schematic lateral view of a generalized uropodid mite showing the structure and position of the endosternite (inset dorsal view) and insertions and origins of the main muscles in the genital area.

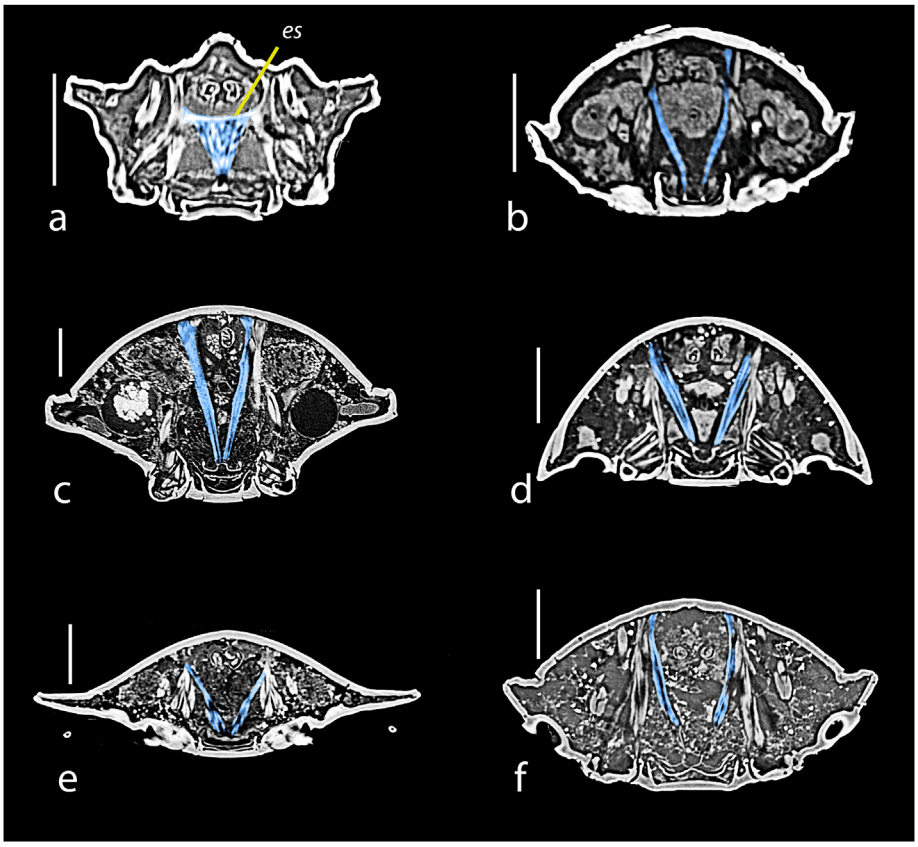

Fig. 8. Cross section of representative Uropodina showing insertion and origin of the levator muscle *m2* (highlighted in blue): a, *Trachytes*; b, *Nenteria*; c, *Uropoda*; d, *Brasiluropoda*; e, *Laqueaturopoda*; f, *Trigonuropoda*. Abbreviations: *es:* endosternite. Scale bars: 100 μm.

taxa with a "durian-style" vagina, they may help open or unfold the vagina.

Aside from the dorsal origins of muscle *m2*, variation was also observed in their insertion points on the endogynium. For instance, in *Trachytes*, *Uropoda* and *Laqueaturopoda*, the two arms of the muscle fuse at one central point in the posterior part, usually the heel of the endogynium (Fig. 8a–c, e). This was also observed in *Metadinychus*, *Australocilliba*, *Acroseius*, *Afrotrachytes*, *Polyaspis*, *Tetrasejaspis* and *Foveolaturopoda*. In most of the remaining taxa, the two arms of the muscle do not fuse but are inserted on two parallel arms of the heel as seen in, e.g., *Brasiluropoda*, *Nenteria*, and *Trigonuropoda* (Fig. 8b–d, f). In some cases, the muscle's insertion is unclear due to an egg obstructing the genital chamber (e.g., *Circocylliba*, *Origmatrachys, Trachycilliba, Trichouropoda,* and all e Rotundabaloghiidae).

Muscle *m3* (the vagina muscle of Michael, dilator of the vaginal cavity (*mva2*) of Akimov and Yastrebsov, not listed by Woodring and Galbraith) inserts ventrally on the distal end of the vagina with

an origin on the ventral shield, close to the anus (Fig. 7). Contraction of this muscle dilates the vagina during oviposition.

Finally, muscle *m4* (retractor muscle of receptaculum seminis of Micheal, not listed by Akimov and Yastrebsov, seminal receptacle constrictor (*Msv*) of Woodring and Galbraith), if present, inserts on the posterior end of the seminal receptacle with an origin on the ventral shield posterior to the origins of *m3* (Fig. 7). Contraction of this muscle is assumed (Michael, 1890; Woodring and Galbraith, 1976) to squeeze the seminal receptacle, thereby releasing some sperm into the atrium.

In many specimens, only a single or a single pair of muscle(s) originating on the ventral shield is attached to structures in the genital atrium. Determining whether these are homologous to *m3* or *m4* is not always straightforward. In some cases, these muscles appear to be attached to the endogynium 2 thus functioning as Michael's *m3* (Fig. 9a–c). In others the insertion of the muscle, near the sperm receptacle, more closely resembles an *m4*. Only in two of the species studied, *Uroobovella luzonensis* and *Cyllibula*, did we observe muscles inserted to both the vagina and sperm receptacle. In these species, the muscles inserted to the vagina originate from the sperm receptacle and not the ventral shield. These observations suggest that the *m3* and *m4* muscles might have a common origin. This is consistent with Woodring and Galbraith (1976) and Akimov and Yastrebtsov (1988) who mentioned only two muscles associated with the genital structures, one each originating from the dorsal and ventral shields.

Variations were also observed in the relative width of paired (or fused) *m3* or *m4* muscles as seen in Fig. 9. The width varied regardless of whether the muscle was attached to the vagina or to the sperm receptacle. For example, in *Brasiluropoda* and *Uroactinia* the muscle functions as an *m4* (Fig. 9d and e) but it has a relatively greater width at both the origin and the insertion points in *Brasiluropoda*. Similarly, in *Uropoda* and *Trigonuropoda* the muscle functions as an *m3* (Fig. 9b–f) but it is much stronger in *Trigonuropoda*. Although most taxa show paired *m3* or *m4* muscles (Fig. 9b–d-f) with separate insertion points these muscles can be fused into a single mass at the point of insertion as observed in *Australocilliba* (*m3*) (Fig. 9c) and *Afrotrachytes* (*m4*) (Fig. 9a).

4.3. Endosternite

The generalized structure of an acarine/parasitiform endosternite consists of a central plate and two pairs of arms extending posteriorly and anteriorly from the central plate (Young, 1970; Akimov and Yastrebtsov, 1988; Evans, 1992) (Fig. 7, inset). In uropodines, development of the endosternite varies from a mostly complete structure with all basal parts present to a strongly reduced structure, featuring a pair of thin arms with no visible central plate. Among the taxa examined, the endosternite of *Afrotrachytes* is most complete featuring both a central plate and well-developed posterior and anterior arms. In this species, the anterior arms are long and associated with dorso-ventral muscles of the coxae. The central plate is wide laterally, tapering slightly towards the center. A largely complete endosternite has also been observed in *Acroseius* and *Polyaspis* with a slight reduction in the development of the posterior arms. A more reduced form has been observed in *Australocilliba*, *Metadinychus*, and *Trachytes*, where the median plate has been modified to a very thin bar. In most remaining species, the endosternite has been reduced to a pair of arms with varying thickness resembling rods rather than plates.

As mentioned above, the endosternite plays a vital role in the attachment of vaginal muscle *m2*. For example, in *Trachytes* (Fig. 8a) where the median plate is reduced to a thin hyaline bar, muscle *m2* originates from the whole width of the bar down to its insertion on endogynium 1 (Fig. 8a). In other uropodines where the endosternite is reduced to two separate parallel rods (arm remnants), muscle *m2* attaches directly to the dorsal shield while "passing" through these rods (Fig. 8b–f).

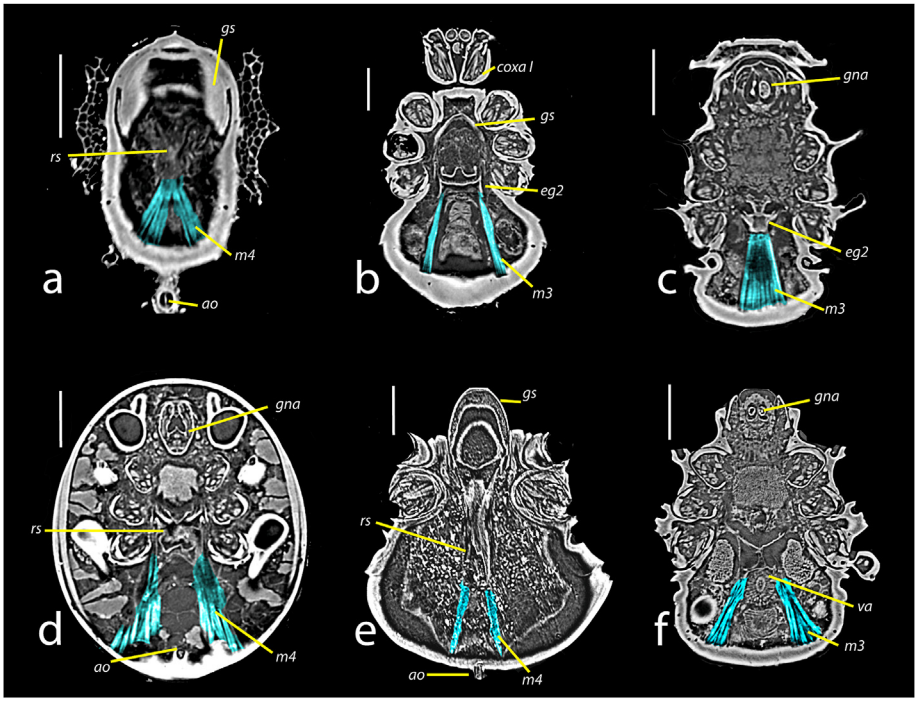

Fig. 9. Longitudinal, horizontal section of representative Uropodina showing insertion and origin of the muscles *m3* or *m4* (highlighted in turquoise) a, *Afrotrachytes*; b, *Uropoda*; c, *Australocilliba*; d, *Brasiluropoda*; e, *Uroactinia*; f, *Trigonuropoda*. Abbreviations: *ao*: anal opening, *eg2*: endogynium 2, *gna*: gnathosoma, *gs*: genital shield, *rs*: sperm receptacle, *va*: vagina. Scale bars: 100 μm.

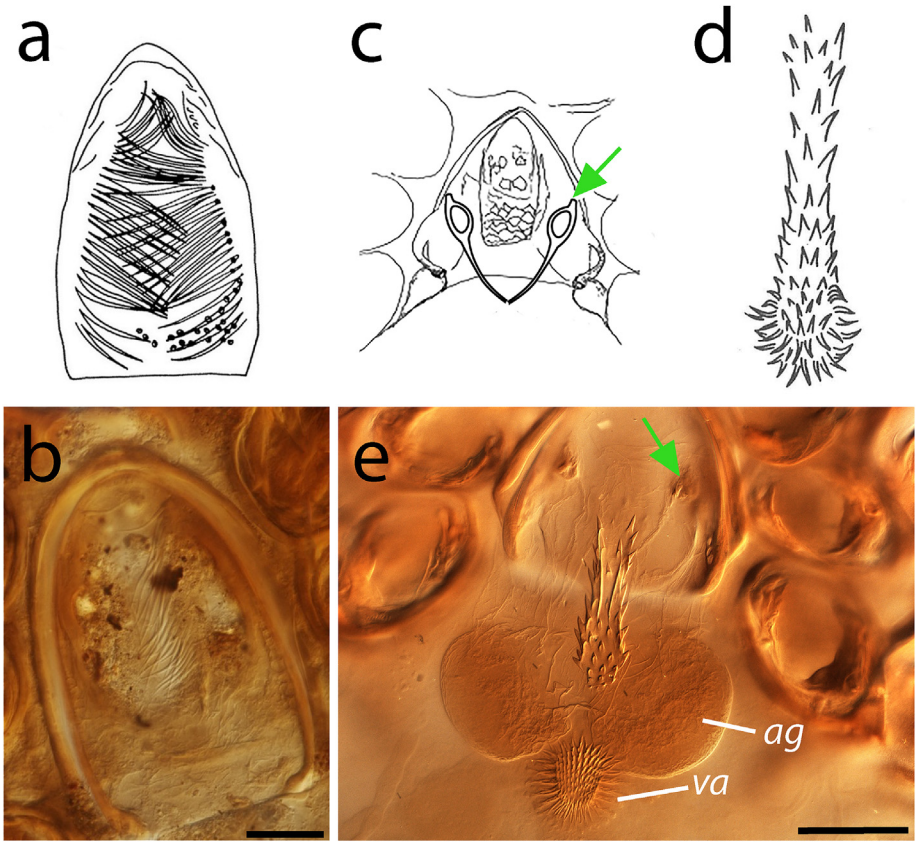

Fig. 10. Female genital atrium structures based on observations using light microscopy. a, drawing of the spine patterns on the chitinized membrane of the endogynium in *Graecatrachys endrodyi* (Hirschmann) (from Hirschmann, 1976f); b, same in photomicrograph of Trachyuropodidae (OSAL 431194); c, Eutrachytidae (specimen from Brazil, image credit MMV); d, connector between vagina and remnant endogynium 1 in *Foveolatatrigon cruzae* (Hirschmann and Hiramatsu) (from Hirschmann and Hiramatsu, 1990); e, connector and durian style vagina in *Trigonuropoda* sp. (OSAL 162400). Red arrows in c and e: "sewing needle-like" rods of endogynium 1. Abbreviations: *ag*: accessory gland, *va:* vagina. Scale bars: 50 μm.

4.4. Associated structures

Other structures recovered from micro-CT data include the membrane lying above the genital shield (*lamina* of Michael), sperm receptacle, and accessory glands (Fig. 7). In some cases, the uterus, oviducts, and fertilized eggs were also easily recognizable in the volumetric data. All species had the lamina which is the structure that lies between the genital shield and the endogynial structures. In contrast, the presence and structure of both the sperm receptacle and the accessory glands varied with some species having both while others lacked one or both.

As with muscle *m4*, not all specimens had a recognizable sperm receptacle. It was absent or poorly developed in *Australocilliba, Nenteria, Trematurella, Trichocylliba, Trigonuropoda, Urodiaspis,* and *Uropoda.* On the other hand, some samples showed a distinct sperm receptacle that appeared to have a spermatophore inside them. This was evident in *Chiropturopoda*, *Trichouropoda*, *Uroobovella luzonensis,* and as the balloon-like structure in some species with durian-type vagina (e.g., *Elegansovella, Micherdzinskiiobovella,* and *Monstrobovella*).

The presence of paired accessory glands was confirmed in females of 14 species among the examined specimens. In these specimens, the glands are easily recognizable and appear as a dense mass in x-ray views. As noted by Michael (1890) the relative size and shape of the paired accessory glands varied across the uropodines, ranging from elongate (e.g. *Dinychus, Leonardiella*) to globular (e.g. *Laqueaturopoda*) or irregular (e.g. *Chiropturopoda, Cyllibula, Trigonuropoda*). The presence of these glands could not be confirmed in the remaining taxa.

4.5. Light microscopy

A number of uropodine species descriptions have documented elements of endogynial structures, but generally without any discussion of the relationship between the observed structures and broader systems or functions. In general, observations based on light microscopy do not include many details on the framework of the endogynium, muscles, or vaginal structures, but light microscopy does reveal some other structures that are poorly or not at all visible using micro-CT. The most obvious of these structures involves the pattern of spines on the membrane of the "sole". Those patterns were noted and described by Michael (Fig. 1, pg), but are difficult to discern in micro-CT, probably because the membranes and spines are very thin.

A couple of different patterns can be distinguished based on those previous descriptions and new observations. Many taxa show the arrangement noted by Michael in various Trematuridae, where small spines are arranged in a specific pattern on what we assume to be the ventral membrane of the endogynial sole. We found variants of this type of pattern in the families Brasiluropodidae, Castriidinychidae, Cillibidae, Nenteriidae, and Uroactiniidae. Some Trematuridae and Uroactiniidae also show a pair of parallel lateral rods which seem to match the lateral support rods of the sole.

The most spectacular (and also most commonly recorded) patterns are found in some genera of Trachyuropodidae. Species in the genera *Graecatrachys*, *Origmatrachys*, *Trachyuropoda*, and *Urojanetia*

show large combs of finger-like structures pointing inward, in some species overlapping medially (Fig. 10a). The combs appear to be inserted on the lateral rods of the endogynial sole. Similar, but shorter and non-overlapping combs have been illustrated for e.g. *Leiodinychus* species (e.g. Michael, 1889; Hiramatsu, 1978).

Descriptions of female genital structures in other genera show only the two parallel rods which we interpret as the lateral support rods of the endogynial sole. This condition seems to be common in Oplitidae.

Taxa that have a reduced endogynium and a durian-style vagina also show specific structures in light microscopy. First among these is the durian-style vagina itself. Often dislodged during slide making, it is among the structures that are distinct in both light microscopy (Fig. 5) and micro-CT. However, light microscopy, especially at high (1000×) magnification, illustrates the intricate folding pattern resulting in the spine-like appearance of the vagina more clearly. A second, far less commonly documented structure was illustrated for *Foveolatatrigon cruzae*(Hirschmann and Hiramatsu) and *Dinychopsis fibulata* (Hirschmann and Zirngiebl-Nicol) (Hirschmann and Zirngiebl-Nicol, 1972; Hirschmann and Hiramatsu, 1990). As usual, the structure reproduced as Fig. 10d was illustrated without comment. Based on results from the micro-CT study, this is most likely the posterior part of the membranous lamina (Fig. 4), folded into a tube that connects the (durian-style) vagina to the remnants of endogynium 1. As with the pattern of spines on the membrane of the "sole" (see above), micro-CT images and 3D modeling fail to render accurate images of the spine patterns on this structure, which is usually easily seen in light microscopy of e.g. *Trigonuropoda* species (Fig. 10e).

5. Discussion

5.1. Structure and variability of the female genital atrium

The current study demonstrated that the structure of the genital atrium and associated features is highly variable among Uropodina. However, a general framework, able to accommodate all observed variants, could be generated. Given this framework, any observations on internal structures in the female genital area using e.g. light microscopy, can now be put in context, increasing their value (e.g. in taxonomic and physiological studies).

The most surprising difference among the studied Uropodina is between those species that show a clear endogynium and a fairly "normal" looking vagina and those that appear to lack well-developed endogynial structures but have gained a "durian-style" vagina. Although some basal taxa (e.g. *Afrotrachytes*, *Trachytes*) show a combination of a poorly developed endogynium and a poorly developed durian-style vagina (see below), the "higher" Uropodina (for the purpose of this study, this includes those taxa characterized by the presence of a sclerotized node on the chelicera; see Table 1) seem to have only one or the other, without intermediates. We hypothesize that the presence of a durian-style vagina (the most easily recognizable structure in light microscopy) most likely indicates presence of the entire alternative system (type 5: reduced endogynial structures, modified muscle attachments, etc.), although this hypothesis needs additional testing. Based on this, our results suggest the existence of two diagnosable lineages in the "higher" Uropodina, one group with a durian-style vagina (Eutrachytidae, Trigonuropodidae, some Urodinychidae), the other with a well-developed endogynium (Cyllibullidae, Nenteriidae, Oplitidae, Trachyuropodidae, Trematuridae, Uroactiniidae, most Urodinychidae). Not all taxa can be accommodated in this system. For example, available data are insufficient to confidently assign *Tetrasejaspis*, *Macrodinychus*, and *Urodiaspis* to either group.

One specific issue affected by these observations concerns the status of the family Urodinychidae (= Ganggattung *Uroobovella* of Hirschmann (1989)). The new observations suggest that this concept of the family may not be monophyletic. Notably, the two broad groupings as defined by development of the endogynium and vagina are also separated by the shape of the chelicera and sternal hypertrichy. Specifically, taxa with a well-developed endogynium usually have extremely elongate chelicera with distinct annulations as well as sternal hypertrichy, while urodinychids with a durian-style vagina have much shorter chelicera without annulations and also lack sternal hypertrichy.

All of this supports the idea that Urodinychidae as currently defined is polyphyletic. The type genus for Urodinychidae, *Urodinychus* Berlese was not examined in this study, but lacks sternal hypertrichy and extreme elongation of the chelicera, suggesting affinities with the smaller lineage with a durian-style vagina (including *Elegansovella*, *Micherdzinskiiobovella*, and *Monstrobovella* based on the current study). Although these hypotheses need to be tested using larger datasets and more taxa, the current observations suggest considerable phylogenetic value of the internal structures examined.

5.2. Function of the internal genital structures relative to mating and oviposition

This study did not include specific observations on function, but our observations do allow an evaluation of some previously proposed hypotheses. Michael (1889) proposed that the spine arrangement on the sole of the endogynium of *L. orbicularis* might serve to strip the chorion of the egg prior to birth of the larva (assuming ovovivipary based on the presence of well-developed larvae in eggs still in the female, and his inability to find eggs in a culture). Subsequently, based on his observations on *O. ovalis* and *P. vegetans* he rejected that hypothesis (Michael, 1890), as these two species have less developed larvae inside females and different arrangements of endogynial spines. The spine patterns on the endogynial sole in Trachyuropodidae are almost species specific, consistent with a function associated with species recognition and mating, rather with oviposition, although the mechanism of such function is currently unclear.

Second, the "durian-style" vagina (Fig. 5). At first glance, it seems well suited to expand for the rather large eggs most uropodids produce, but members of the lineage having a well-developed endogynium have similarly sized eggs but lack this modification of the vagina (they have well developed circular muscles surrounding the vagina). These observations are inconsistent with the hypothesis that the durian style vagina evolved to accommodate large eggs. Given this, we assume that the observed modifications (presence of a well-developed endogynium or a well-developed "durian-style" vagina) are associated with mating and processing of the spermatophore, rather than with oviposition. Additional data that we believe to be relevant concerns the mating mode in "higher" uropodines (Radinovsky, 1965; Faasch, 1967; Athias-Binche, 1981; Marquardt and Kaczmarek, 2013; Vázquez et al., 2022). In these groups, males produce an ectospermatophore which is glued to the outside of the female genital shield. From this ectospermatophore a thin tube emerges (the endospermatophore) which enters the genital atrium and presumably releases the sperm either in the atrium or in the seminal receptacle. In lower uropodines (e.g. *Uropoda orbicularis*, Uropodidae) males may be guiding the endospermatophore by inserting their chelicera in the genital atrium (Faasch, 1967), but although males and females in "higher" uropodines (Trematuridae, Uroactiniidae, Urodinychidae) manipulate the spermatophore and female genital shield area with their palps, there is no evidence of insertion of

chelicera (Faasch, 1967; Athias-Binche, 1981; Marquardt and Kaczmarek, 2013; Vázquez et al., 2022).

This leaves the question of how the endospermatophore is oriented towards the genital atrium. Woodring and Galbraith (1976) proposed that the rapid opening of the genital shield and/or rapid elevation of the endogynium might create some sort of vacuum, effectively "sucking" the endospermatophore into the genital atrium. In this context it is worthwhile to repeat that although the entire genital shield is lowered, the opening to the external environment is restricted to the anterior end. The lateral areas are sealed off by unfolding membranes. The "durian-style" vagina might serve the same purpose: by rapidly expanding it might "suck in" the endospermatophore. The musculature for such a process appears to be present. The strong muscle *m2* is attached to the heel of the endogynium and can raise the endogynium. As for the durian style vagina, a combination of muscles *m3*, pulling the anterior end of the sclerotized tube in the vagina and muscle *m2*, pulling the membrane of the genital atrium by the needle like rods, might cause a rapid unfolding of the structure (the vagina is ectodermal and has a cuticle, presumably making it sufficiently stiff to allow rapid unfolding to create a vacuum in the genital atrium).

A final question might be how such complex systems may have evolved. A possible clue is found in several of the "lower" Uropodina (e.g. *Afrotrachytes*, *Trachytes*). In these taxa we found evidence of a poorly developed endogynium (relatively smaller endogynium 1 and generally flat endogynium 2) and a poorly developed durian-style vagina (fewer and less compact folds). This suggests that both structures may have developed for different reasons and were co-opted for a different function in the two lineages of "higher" uropodines. Admittedly, these hypotheses are speculative, but they are consistent with available evidence.

5.3. Complementary of micro-CT and light microscopy

Synchrotron-based micro-CT (SR-μCT) proved to be valuable for visualizing the 3D morphology of uropodid mites but does not resolve all issues. Therefore, we employed the more traditional light microscopy as a complementary technique. For example, Michael stated that the membrane making up the bulk of the endogynium was chitinized, but micro-CT did not allow consistent recognition of this structure. In contrast, the spines on the membrane of the endogynial sole (Fig. 10a and b) or lamina (Fig. 10d and e) (when present) can be seen fairly easily using light microscopy. On the other hand, the structure of the sclerotized lateral margins of the endogyniums can usually not be reconstructed using light microscopy of slide mounted specimens but is distinct in our micro-CT images. One complication in integrating micro-CT results with observations based on light microscopy is the highly biased selection of taxa for which light microscopy-based data are available. Illustrations are largely restricted to taxa with very distinct features (e.g. *Trachyuropoda*, Fig. 10a). In contrast, species with very small or weakly developed structures in this area are rarely illustrated. These omissions need to be rectified to get a more complete understanding of variability in the female genital atrium across Uropodina.

CRediT authorship contribution statement

Jeremy Naredo: Writing – review & editing, Writing – original draft, Visualization, Methodology, Investigation, Data curation, Conceptualization. **J. Orlando Combita-Heredia:** Visualization, Software, Resources, Methodology, Data curation, Conceptualization. **Thomas van de Kamp:** Writing – review & editing, Resources, Investigation. **Marcus Zuber:** Writing – review & editing, Software, Resources. **Elias Hamann:** Writing – review & editing, Software, Resources. **Ma. Magdalena Vázquez:** Visualization, Resources, Investigation. **Hans Klompen:** Writing – review & editing, Writing – original draft, Visualization, Validation, Supervision, Project administration, Funding acquisition, Conceptualization.

Data availability

All processed tomograms (TIFF z-stacks) are archived at the RADAR4KIT (https://doi.org/10.35097/0u46gbjp0eagttk1).

Funding

The project was funded in part through U.S. National Science Foundation grant DEB2017439.

Declaration of competing interest

The authors declare that they have no known competing financial interests or personal relationships that could have appeared to influence the work reported in this paper.

Acknowledgements

We thank Tomáš Faragó (KIT) for the tomographic reconstructions, Ian Brackett (OSU) for initial data cropping, and Antonella di Palma (Università degli studi di Foggia) for discussions on internal anatomy. We acknowledge the KIT Light Source for the provision of instruments at their beamlines and thank the Institute for Beam Physics and Technology (IBPT) for the operation of the Karlsruhe Research Accelerator (KARA).

References

Akimov, I.A., Yastrebtsov, A.V., 1988. Skeletal-muscular system of gamasid mites (Mesostigmata: Gamasina). Zool. Jahrb., Abt. Anat. Ontog. Tiere 117, 397–439.

Alberti, G., Coons, L.B., 1999. Volume C. Acari: Mites. In: Harrison, F.W., Foelix, R.F. (Eds.), Microscopic Anatomy of Invertebrates, Chelicerate Arthropoda, vol. 8. John Wiley & Sons, Inc., New York, NY, pp. 515–1215.

Alberti, G., Di Palma, A., 2002. Fine structure of the phytoseiid-type sperm access system (Acari, Gamasida, Phytoseiidae). In: Bernini, F., Nannelli, R., Nuzzaci, G., De Lillo, E. (Eds.), Acarid Phylogeny and Evolution: Adaptation in Mites and Ticks. Kluwer Academic Publishers, Siena, Italy, pp. 241–252.

Alberti, G., Gegner, A., Witalinski, W., 1999. Observations on the fine structure of the vagina of pergamasid mites (Pergamasidae, Parasitina, Gamasida). In: Bruin, J., Geest, L.P.S., der, van, Sabelis, M.W. (Eds.), Evolution and Ecology of Acari. Kluwer Academic Publishers, Amsterdam, pp. 593–601.

Athias-Binche, F., 1981. Contribution a la connaissance des uropodides libres (Arachnides: Anactinotriches) de quelque écosystèmes forestiers européens. Univ. P. M. Curie Paris VI, Paris, p. 308.

Beaulieu, F., Dowling, A.P.G., Klompen, H., Moraes, G.J., de Walter, D.E., 2011. Superorder Parasitiformes Reuter, 1909. In: Zhang, Z.-Q. (Ed.), Animal Biodiversity: an Outline of Higher-Level Classification and Survey of Taxonomic Richness. Zootaxa, pp. 123–128.

Bhattacharyya, S.K., 1963. A revision of the British mites of the genus *Pergamasus* Berlese s. lat. (Acari: Mesostigmata). Bull. Br. Mus. Nat. Hist. Zool. 11, 131–242 plates 131-138.

Blender_Development_Team, 2024. Blender [Computer software], Version 4.1.

Boudinot, B.E., van de Kamp, T., Peters, P., Knöllinger, K., 2024. Male genitalia reconsidered: A multimodal anatomy of the bullet ant (*Paraponera clavata*; Hymenoptera, Formicidae). J. Morphol. 285, e21757. https://doi.org/10.1002/jmor.21757.

Cecilia, A., Rack, A., Douissard, P.-A., Martin, T., dos Santos Rolo, T., Vagovič, P., Hamann, E., van de Kamp, T., Riedel, A., Fiederle, M., Baumbach, T., 2011. LPE grown LSO:Tb scintillator films for high resolution X-ray imaging applications at synchrotron light sources. Nucl. Instrum. Methods Phys. Res. 648, S321–S323. https://doi.org/10.1016/j.nima.2010.10.150.

Cómbita-Heredia, O., Gulbronson, C.J., Ochoa, R., Quintero-Gutiérrez, E.J., Bauchan, G., Klompen, H., 2021. Size, shape, and direction matters: Matching secondary genital structures in male and female mites using multiple microscopy techniques and 3D modeling. PLoS One 16, e0254974. https://doi.org/10.1371/journal.pone.0254974.

Di Palma, A., Wegener, A., Alberti, G., 2009. On the ultrastructure and functional morphology of the male chelicerae (gonopods) in Parasitina and Dermanyssina mites (Acari: Gamasida). Arthropod Struct. Dev. 38, 329–338. https://doi.org/10.1016/j.asd.2009.01.003.

Douissard, P.-A., Cecilia, A., Rochet, X., Chapel, X., Martin, T., van de Kamp, T., Helfen, L., Baumbach, T., Luquot, L., Xiao, X., Meinhardt, J., Rack, A., 2012. A versatile indirect detector design for hard X-ray microimaging. J. Instrum. 7, P09016. https://doi.org/10.1088/1748-0221/7/09/P09016.

Evans, G.O., 1992. Principles of Acarology, first ed. CAB International, Wallingford, UK.

Faasch, H., 1967. Beitrag zur biologie der einheimischen Uropodiden *Uroobovella marginata* (C.L. Koch 1839) und *Uropoda orbicularis* (O.F. Müller 1776) und experimentelle Analyse ihres Phoresieverhaltens. Zool. Jahrb., Abt. Syst. 94, 521–608.

Faragó, T., Gasilov, S., Emslie, I., Zuber, M., Helfen, L., Vogelgesang, M., Baumbach, T., 2022. Tofu: a fast, versatile and user-friendly image processing toolkit for computed tomography. J. Synchrotron Radiat. 29, 916–927. https://doi.org/10.1107/S160057752200282X.

Faulwetter, S., Vasileiadou, A., Kouratoras, M., Dailianis, T., Arvanitidis, C., 2013. Micro-computed tomography: Introducing new dimensions to taxonomy. ZooKeys 263, 1–45. https://doi.org/10.3897/zookeys.263.4261.

Fedorov, A., Beichel, R., Kalpathy-Cramer, J., Finet, J., Fillion-Robin, J.-C., Pujol, S., Bauer, C., Jennings, D., Fennessy, F., Sonka, M., Buatti, J., Aylward, S., Miller, J.V., Pieper, S., Kikinis, R., 2012. 3D Slicer as an image computing platform for the Quantitative Imaging Network. Magn. Reson. Imaging 30, 1323–1341. https://doi.org/10.1016/j.mri.2012.05.001.

Hiramatsu, N., 1978. Gangsystematik der Parasitiformes. Teil 263. Teilgang einer neuen *Trichouropoda*-Art der *Orbicularis*-Gruppe aus Japan (Trichouropodini, Uropodinae). Acarologie 24, pp. 19–20.

Hirschmann, W., 1976a. Gangsystematik der Parasitiformes. Teil 216. 3 neue *Trachyuropoda*-Arten der *Magna*-Gruppe. Acarologie (Nuremberg) 22, 16–18.

Hirschmann, W., 1976b. Gangsystematik der Parasitiformes. Teil 217. 4 neue *Trachyuropoda*-Arten der *Coccinea*-Gruppe. Acarologie (Nuremberg) 22, 18–21.

Hirschmann, W., 1976c. Gangsystematik der Parasitiformes. Teil 219. 2 neue *Trachyuropoda*-Arten der *Multituberosa*-Gruppe. Acarologie (Nuremberg) 22, 23–24.

Hirschmann, W., 1976d. Gangsystematik der Parasitiformes. Teil 221. 1 neue *Trachyuropoda*-Art der *Troguloides*-Gruppe (Trachyuropodini, Oplitinae). Acarologie (Nuremberg) 22, 25–26.

Hirschmann, W., 1976e. Gangsystematik der Parasitiformes. Teil 222. 1 neue Trachyuropoda-Art der Berlesiana-Gruppe. Acarologie 22, 26–27.

Hirschmann, W., 1976f. Gangsystematik der Parasitiformes. Teil 224. 6 neue *Trachyuropoda*-Arten der *Graeca*-Gruppe. Acarologie (Nuremberg) 22, 30–34.

Hirschmann, W., 1976g. Gangsystematik der Parasitiformes. Teil 225. 6 neue *Trachyuropoda*-Arten der *Festiva*-Gruppe. Acarologie (Nuremberg) 22, 34–39.

Hirschmann, W., 1976h. Gangsystematik der Parasitiformes. Teil 226. 9 neue *Trachyuropoda*-Arten der *Origmophora*-Gruppe. Acarologie (Nuremberg) 22, 39–44.

Hirschmann, W., 1976i. Gangsystematik der Parasitiformes. Teil 227. 1 neue Trachyuropoda-Art der Lindquisti-Gruppe. Acarologie 22, 44–45.

Hirschmann, W., 1989. Gangsystematik der Parasitiformes. Teil 509, Die Gangattung *Uroobovella* Berlese 1903 -Artengruppen - Bestimmungstabellen - Diagnosen - (Dinychini, Uropodinae). Acarologie (Nuremberg) 36, 84–196.

Hirschmann, W., Hiramatsu, N., 1990. Gangsystematik der Parasitiformes. Teil 527, Zwölf neue *Trigonuropoda*-Arten der *difoveolata*- und *trichokaszabia*-Gruppe aus Formosa und den Philippinen (Dinychini, Uropodinae). Acarologie (Nuremberg) 37, 149–169.

Hirschmann, W., Zirngiebl-Nicol, I., 1972. Gangsystematik der Parasitiformes. Teil 127. Teilgänge, Stadien von 19 neuen *Uroobovella*-Arten (Dinychini, Uropodinae). Acarologie (Nuremberg) 18, 110–119.

Kazemi, S., Klompen, H., Moraza, M.L., Kamali, K., Saboori, A., 2008. A new species of *Weiseronyssus* Samsinak 1962 (Acari: Mesostigmata: Diplogyniidae) from Iran, with a key for genera. Zootaxa 1824, 17–27.

Keklikoglou, K., Arvanitidis, C., Chatzigeorgiou, G., Chatzinikolaou, E., Karagiannidis, E., Koletsa, T., Magoulas, A., Makris, K., Mavrothalassitis, G., Papanagnou, E.-D., Papazoglou, A.S., Pavloudi, C., Trougakos, I.P., Vasileiadou, K., Vogiatzi, A., 2021. Micro-CT for Biological and Biomedical Studies: A Comparison of Imaging Techniques. J. Imaging 7, 172. https://doi.org/10.3390/jimaging7090172.

Kontschán, J., 2024. Uropodina genera of the world. Inform, Kiadó és Nyomda Kft, Budapest, p. 241.

Lieberman, Z., Billen, J., van de Kamp, T., Boudinot, B.E., 2022. The ant abdomen: the skeletomuscular and soft tissue anatomy of *Amblyopone australis* workers (Hymenoptera: Formicidae). J. Morphol. 283, 693–770. https://doi.org/10.1002/jmor.21471.

Lösel, P.D., van de Kamp, T., Jayme, A., Ershov, A., Faragó, T., Pichler, O., Jerome, N.T., Aadepu, N., Bremer, S., Chilingaryan, S.A., Heethoff, M., Kopmann, A., Odar, J., Schmelzle, S., Zuber, M., Wittbrodt, J., Baumbach, T., Heuveline, V., 2020. Introducing Biomedisa as an open-source online platform for biomedical image segmentation. Nat. Commun. 11. https://doi.org/10.1038/s41467-020-19303-w.

Marquardt, T., Kaczmarek, S., 2013. Mating behaviour of *Trichouropoda ovalis* (Acari: Mesostigmata: Uropodina: Trematuridae) with notes on phylogeny of reproductive biology in the Parasitiformes. Int. J. Acarol 39, 369–376. https://doi.org/10.1080/01647954.2013.800133.

Meira, O.M., Beutel, R.G., Pohl, H., van de Kamp, T., Almeida, E.A.B., Boudinot, B.E., 2024. Bee morphology: A skeletomuscular anatomy of *Thyreus* (Hymenoptera: Apidae). J. Morphol. 185, e21751. https://doi.org/10.1002/jmor.21751.

Metscher, B.D., 2009. MicroCT for comparative morphology: Simple staining methods allow high-contrast 3D imaging of diverse non-mineralized animal tissues. BMC Physiol. 9, 11. https://doi.org/10.1186/1472-6793-9-11.

Michael, A.D., 1889. Observations on the Special Internal Anatomy of *Uropoda krameri*. J. R. Microsc. Soc. 9, 1–15. https://doi.org/10.1111/j.1365-2818.1889.tb05844.x. + 11 plate.

Michael, A.D., 1890. On the variations of the female reproductive organs, especially the vestibule, in different species of *Uropoda*. J. R. Microsc. Soc. 10, 142–152. https://doi.org/10.1111/j.1365-2818.1890.tb00789.x.

Michael, A.D., 1894. Notes on the Uropodinae. J. R. Microsc. Soc. 14, 289–319. https://doi.org/10.1111/j.1365-2818.1894.tb00029.x.

Paganin, D., Mayo, S.C., Gureyev, T.E., Miller, P.R., Wilkins, S.W., 2002. Simultaneous phase and amplitude extraction from a single defocused image of a homogeneous object. J. Microsc. 206, 33–40. https://doi.org/10.1046/j.1365-2818.2002.01010.x.

Radinovsky, S., 1965. The biology and ecology of granary mites of the Pacific Northwest. IV. Various aspects of the reproductive behavior of *Leiodinychus krameri* (Acarina: Uropodidae). Ann. Entomol. Soc. Am. 58, 267–272. https://doi.org/10.1093/aesa/58.3.267.

Schindelin, J., Arganda-Carreras, I., Frise, E., Kaynig, V., Longair, M., Pietzsch, T., Preibisch, S., Rueden, C., Saalfeld, S., Schmid, B., Tinevez, J.-Y., White, D.J., Hartenstein, V., Eliceiri, K., Tomancak, P., Cardona, A., 2012. Fiji: an open-source platform for biological-image analysis. Nat. Methods 9, 676–682. https://doi.org/10.1038/nmeth.2019.

Trägårdh, I., 1950. Studies on the Celaenopsidae, Diplogyniidae and Schizogyniidae (Acarina). Ark. Zool. 1, 361–451.

van de Kamp, T., Mikó, I., Staniczek, A., Eggs, B., Bajerlein, D., Faragó, T., Hagelstein, L., Hamann, E., Spiecker, R., Baumbach, T., Jansta, P., Krogmann, L., 2022. Evolution of flexible biting in hyperdiverse parasitoid wasps. Proc. R. Soc. B Biol. Sc. 289, 20212086. https://doi.org/10.1098/rspb.2021.2086.

van de Kamp, T., Schwermann, A.H., dos Santos Rolo, T., Lösel, P.D., Engler, T., Etter, W., Faragó, T., Göttlicher, J., Heuveline, V., Kopmann, A., Mähler, B., Mörs, T., Odar, J., Rust, J., Tan Jerome, N., Vogelgesang, M., Baumbach, T., Krogmann, L., 2018. Parasitoid biology preserved in mineralized fossils. Nat. Commun. 9, 3325. https://doi.org/10.1038/s41467-018-05654-y.

Vázquez, M.M., May, D., Klompen, H., De Moraes, G.J., 2022. Aspects of the biology, behavior and mating of *Uroactinia* sp. (Acari: Mesostigmata: Uropodina: Uroactiniidae). Syst. Appl. Acarol. 27, 2258–2268. https://doi.org/10.11158/saa.27.11.11.

Vogelgesang, M., Chilingaryan, S.A., dos Santos Rolo, T., Kopmann, A., 2012. UFO: A scalable GPU-based image processing framework for on-line monitoring. 2012 IEEE 14th International Conference on High Performance Computing and Communication & 2012 IEEE 9th International Conference on Embedded Software and Systems, pp. 824–829. https://doi.org/10.1109/HPCC.2012.116.

Vogelgesang, M., Faragó, T., F, M.T., Helfen, L., dos Santos Rolo, T., Myagotin, A., Baumbach, T., 2016. Real-time image-content-based beamline control for smart 4D X-ray imaging. J. Synchrotron Radiat. 23, 1254–1263. https://doi.org/10.1107/S1600577516010195.

Wolf, I., Vetter, M., Wegner, I., Nolden, M., Bottger, T., Hastenteufel, M., Schobinger, M., Kunert, T., Meinzer, H.-P., 2004. The medical imaging interaction toolkit (MITK): A toolkit facilitating the creation of interactive software by extending VTK and ITK. Proc. SPIE 5367. https://doi.org/10.1117/12.535112. Visualization, Image-Guided Procedures, and Display.

Woodring, J.P., Galbraith, C.A., 1976. The anatomy of the adult uropodid *Fuscouropoda agitans* (Arachnida: Acari), with comparative observations on the other Acari. J. Morphol. 150, 19–58. https://doi.org/10.1002/jmor.1051500103.

Young, J.H., 1970. The muscles and endosternum of *Haemogamasus ambulans*. Can. Entomol. 102, 157–163.